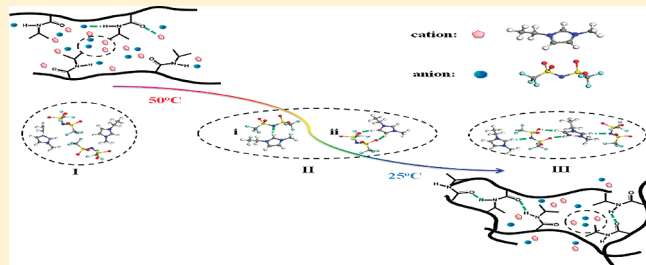


Spectral Insights into Gelation Microdynamics of PNIPAM in an Ionic Liquid

Zhangwei Wang and Peiyi Wu*

The Key Laboratory of Molecular Engineering of Polymers, Ministry of Education, Department of Macromolecular Science, and Laboratory of Advanced Materials, Fudan University, Shanghai 200433, People's Republic of China

ABSTRACT: The gelation microdynamic mechanism of PNIPAM in a ionic liquid, 1-ethyl-3-methylimidazolium bis(trifluoromethylsulfonyl)imide ($[C_2\text{mim}][\text{NTf}_2]$), is investigated by FTIR spectroscopy in combination with two-dimensional correlation spectroscopy (2Dcos) and perturbation correlation moving window (PCMw) technique for the first time. Appreciable changes in band frequencies and shapes are observed in the $\nu(\text{N}-\text{H})$ and $\nu(\text{C}=\text{O})$ regions, indicating the formation of new interactions between the ionic liquid and PNIPAM and the transformation of interior interaction between polymer chains during gelation. In particular, the variation of the ion environment with the relative change of the isolated and associated components of $[C_2\text{mim}][\text{NTf}_2]$ on the sol-to-gel transition of PNIPAM is revealed by 2DIR analysis to the $\nu(\text{C}-\text{H})$ region of imidazole ring. Upon cooling, the side chains of PNIPAM experience a changing process from dissociation of the interaction with ionic liquid to formation of $\text{N}-\text{H}\cdots\text{O}=\text{C}$ hydrogen bonding, then polymer shrinks from the side chains to backbone, followed by the final immobilization of the associated species in polymer network. Meanwhile, the gelation is actually a desolvation process upon the variation of ion environment.



1. INTRODUCTION

Ionic liquids (ILs) are recognized as a “green” (environmentally friendly) alternative to the traditional inorganic and organic solvents because of their unique properties (such as negligible vapor pressures, high thermal stabilities, wide electrochemical window, and excellent ionic conductivities),^{1–3} which are flexibly tuned through combination of anion and cation, with numerous ion pairs possible.⁴ Because ILs are entirely composed of ions, the existing form of ions is fundamentally important to describe the feature of ILs. Previously, an indication of ion-pair, cluster formation, or both in imidazolium-based ILs was reported, such as 1-ethyl-3-methylimidazolium bis(trifluoromethanesulfone)-imide ($[C_2\text{mim}][\text{NTf}_2]$),⁵ and further investigations revealed the evidence of strongest hydrogen bond involving the most acidic $C_2-\text{H}$ of the imidazolium cation, followed by $C_4-\text{H}$ and $C_5-\text{H}$.^{6–8} The degree of formation of ion pairs or hydrogen-bonded clusters can be modulated by temperature,^{5,9} pressure,¹⁰ ionic medium,¹¹ hydration,¹¹ and added polymers.^{5,10} Jiang et al. found that the addition of triblock PEO–PPO–PEO copolymers to 1-ethyl-3-methylimidazolium bis(trifluoromethylsulfonyl)amide ($[\text{EMIM}][\text{TFSA}]$) leads to the formation of $\text{C}-\text{H}\cdots\text{O}$ interactions between imidazolium $\text{C}-\text{H}$ groups and oxygen atoms of polyethylene oxides (PEOs).¹⁰ With the change of relative components of the isolated and associated species of ILs, the solvation in ILs is of interest.

Furthermore, because of the excellent properties of ILs, especially the negligible vapor pressures and the high ionic conductivity, many previous works have shed light on the possibility to take them as gelation solvents in electrochemical

field, immediately expanded to lithium ion batteries, capacitors, and fuel cell electrolytes.^{3,12,13} Recently, most studies on the combined use of ILs with polymers have dealt with polymerization in IL solvents;¹² however, several studies on the utilization of the phase changes or phase separation of a polymer in an IL have been represented, which are much more simply prepared, tunable, and eco-friendly.^{13,14} The sol–gel transition of polymers in ILs has been paid attention to fabricate polymer electrolyte. Polymer gels containing poly(vinylidene fluoride)–hexafluoropropylene copolymer (P(VdF-co-HFP)) and imidazolium-based ILs with high ionic conductivity have been widely investigated, and the gelation is probably caused by the growth of spherulites upon cooling.^{15–17} Harner et al. also prepared gels by crystallization of poly(ethylene glycol) (PEG) dissolved in a room-temperature ionic liquid 1-ethyl-3-methylimidazolium ethylsulfate ($[\text{EMIM}][\text{EtSO}_4]$);¹⁸ similarly, a cross-linked PEG matrix has been used to gel an IL $[C_6\text{mim}][\text{NTf}_2]$.¹⁹ Besides, Kawauchi et al. successfully obtained thermoreversible IL gels by stereocomplexation of IL-dissolved isotactic and syndiotactic polymethyl methacrylates (PMMA).²⁰ Upon the UCST²¹ and LCST-type^{22,23} behavior for polymers in ILs, Watanabe et al. prepared gels of poly(*N*-isopropyl acrylamide) and poly(benzyl methacrylate) by photoinitiated radical polymerization. Physical gelation by the self-assembly of the block-type in ILs has also been performed. He and Lodge used the ABA triblock copolymers,

Received: June 16, 2011

Revised: August 10, 2011

Published: August 11, 2011

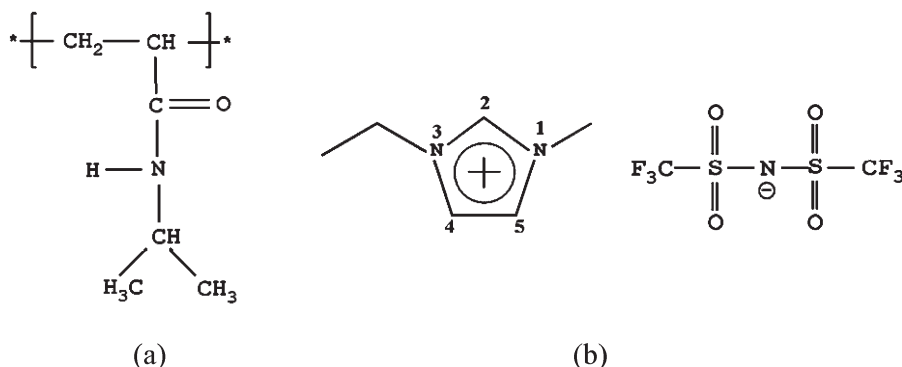


Figure 1. Chemical structure of PNIPAM (a) and 1-ethyl-3-methylimidazolium bis(trifluoromethylsulfonyl) imide ($[C_2\text{mim}][\text{NTf}_2]$) (b).

such as poly(styrene-*b*-ethyleneoxide-*b*-styrene) and poly(*N*-isopropyl acrylamide-*b*-ethylene oxide-*b*-*N*-isopropyl acrylamide), to mix with an IL to get gels on the basis of the different solubility for the A and B blocks in ILs.^{24–26}

On the basis of previous studies, plenty of investigations have been devoted to introduce the new methods to gel as well as the fresh kinds of polymer gels; however, only a few studies have so far been reported for the molecular microdynamics in polymer–IL system during gelation. Dynamic light scattering (DLS) and small-angle neutron scattering (SANS) have been applied to investigate the LCST phase behavior in ILs from a structural aspect.²⁷ Additionally, most of this research is interested in the physical characteristics of polymer gels, such as ionic conductivity, rheological properties, and mechanical properties,^{16,18,24–26} whereas the interactions of polymers with ILs, especially the variation of the ion environment during phase transition, have been limitedly studied.

In the present work, a simple IL gelation scheme is outlined for poly(*N*-isopropylacrylamide) (PNIPAM) in a ionic liquid, 1-ethyl-3-methylimidazolium bis(trifluoromethylsulfonyl)-imide ($[C_2\text{mim}][\text{NTf}_2]$). PNIPAM is the well-known polymer that exhibits a lower critical solution temperature (LCST) behavior in an aqueous solution,^{28–30} whereas an upper critical solution temperature (UCST) behavior in an IL is observed, which is strongly affected by PNIPAM concentration and molecular weight.²¹ At modestly elevated temperature ($>37^\circ\text{C}$), with proper concentration, PNIPAM dissolves in $[C_2\text{mim}][\text{NTf}_2]$, but, at lower temperatures, nontransparent gel forms. In this work, the microdynamics during the phase transition involving the interaction among polymer, cations, and anions, in particular, the variation of the ion composition in ILs, are investigated by Fourier transform infrared spectroscopy (FTIR). As we know, FTIR is an effective method to detect the molecular interactions, especially for the hydrogen bonding interaction,^{5,10} but it is not so effective to improve the spectral resolution by capturing subtle information that is not obvious or overlapped in 1D FTIR spectra. As a supplement, two-dimensional correlation spectroscopy (2Dcos)^{31,32} in combination with perturbation correlation moving window (PCMW)^{33,34} technique was used to obtain information about molecular motions or conformational changes. For PNIPAM aqueous solution, the phase separation mechanism has been studied by FTIR and 2DIR³⁰ as well as for the PNIPAM hydrogel.³⁵ In our work, it is notable that this is for the first time to employ 2DIR to investigate further the molecule-level microdynamics of PNIPAM gel in ILs. Wherein, the variation of the ion environment, such as free ions, ion pairs, and clusters, can be

further confirmed, and the great influence of the variation on the sol-to-gel transition of PNIPAM will be elucidated.

2. EXPERIMENTAL SECTION

2.1. Materials and Synthesis. *N*-Isopropylacrylamide (NIPAM) monomers were purchased from Tokyo Kasei Kogyo (Tokyo, Japan) and further purified before use. PNIPAM was synthesized by free-radical polymerization in tetrahydrofuran (THF) as solvent. The reaction was initiated by azobis(isobutyronitrile) (AIBN) and carried out at 70°C for 12 h under a nitrogen environment. After precipitation by diethyl ether, the product was dried under vacuum to constant weight. The molecular weight of PNIPAM, M_w 1.1×10^4 , and polydispersity index, M_w/M_n 1.6, were measured by a Voyager DE-STR matrix-assisted laser desorption/ionization time-of-flight (MALDI TOF MS) mass spectrometer equipped with a 337 nm nitrogen laser. The ionic liquid, 1-ethyl-3-methylimidazolium bis(trifluoromethanesulfone)imide ($[C_2\text{mim}][\text{NTf}_2]$), was purchased from Sigma-Aldrich (>98%).

Figure 1 shows the chemical structures of the PNIPAM and $[C_2\text{mim}][\text{NTf}_2]$ with three hydrogen atoms on the imidazole ring, which are usually numbered as $C_2\text{--H}$, $C_4\text{--H}$, and $C_5\text{--H}$.

2.2. Sample Preparation. PNIPAM was insoluble in $[C_2\text{mim}][\text{NTf}_2]$ at room temperature, so the mixture of PNIPAM/ $[C_2\text{mim}][\text{NTf}_2]$ with 10 wt % PNIPAM was heated to 60°C for 24 h to achieve dissolution. The fully transparent solution was vacuum-dried at 70°C for an additional 24 h to prevent absorption of atmospheric moisture. During cooling from 70°C to room temperature, the PNIPAM/ $[C_2\text{mim}][\text{NTf}_2]$ solution experienced a kinetically liquid–solid phase transition.

2.3. Fourier Transform Infrared Spectroscopy. The FTIR spectra were recorded with a 4 cm^{-1} spectral resolution on a Nicolet Nexus 470 spectrometer equipped with a DTGS detector by signal-averaging 32 scans. Two pieces of microscope KBr windows, which have no absorption bands in the MIR region, were used to prepare a transmission cell. Temperature-dependent spectra were collected between 50 and 25°C in intervals of 1°C , with an accuracy of 0.1°C . The baseline-corrected processing was performed by the software Omnic 8.0.

2.4. Perturbation Correlation Moving Window. FTIR spectra recorded at an interval of 1°C were selected in the ranges of interest to perform PCMW analysis, and further correlation information was calculated by the software 2D Shige, ver. 1.3 (Shigeaki Morita, Kwansei-Gakuin University, Japan, 2004–2005) with an appropriate window size ($2m + 1 = 11$). Furthermore, the final contour maps were plotted by Origin program, ver. 8.0, with

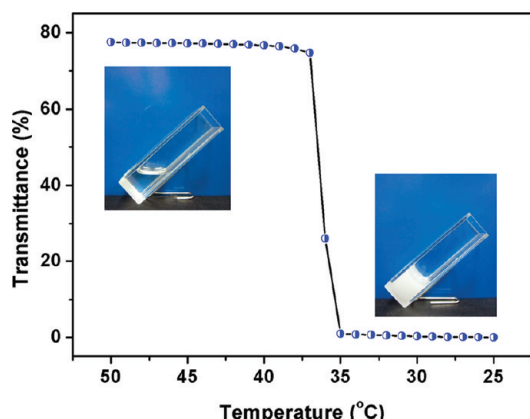


Figure 2. Temperature-dependent transmittance of 10 wt % PNIPAM/[C₂mim][NTf₂] during cooling from 50 to 25 °C with an increment of 1 °C. The insets are photographs of the solution and gel at corresponding temperatures.

red-colored regions defined as positive intensities and green-colored regions defined as negative intensities.

2.5. Two-Dimensional Correlation Analysis. FTIR spectra used for PCMW analysis were also used to perform 2D correlation analysis, and further correlation information was also calculated by the same software 2D Shige, ver. 1.3. Similarly, the final contour maps were plotted by Origin program, ver. 8.0, with red-colored regions defined as positive intensities and green-colored regions defined as negative intensities.

3. RESULTS AND DISCUSSION

3.1. Sol-to-Gel Transition. During cooling from 50 °C to room temperature, the solutions with PNIPAM in [C₂mim][NTf₂] experience phase transition and were examined by turbidity measurement. Note that a proper solution with 10 wt % PNIPAM is chosen in this Article, which has experienced a sol-to-gel transition, forming thermoreversible gel upon mildly cooling. The observed phase behavior of PNIPAM/[C₂mim][NTf₂] cooling from 50 to 25 °C is showed in Figure 2. The *T*_{gel} can be easily determined to be 37 °C; furthermore, the initial transmittance at higher temperature is lower than neat [C₂mim][NTf₂], probably because of the imperfect solubility³⁶ in ILs due to the higher concentration of PNIPAM.

3.2. Conventional IR Analysis. Figure 3 shows the FTIR spectra of [C₂mim][NTf₂], PNIPAM and the PNIPAM/[C₂mim][NTf₂] gel. Seen from the IR spectrum of gel, it is noted that a new band at 3387 cm⁻¹ appears, which should be assigned to the new interaction of PNIPAM and [C₂mim][NTf₂], in the form of the hydrogen bond between the N—H groups and anions of [C₂mim][NTf₂].^{4,37} The existence of PNIPAM is proven by the N—H stretching (3450–3220 cm⁻¹) as well as C=O groups at 1646 cm⁻¹, and [C₂mim][NTf₂] showed up by the bands around 3150 cm⁻¹, which come from stretching vibrational modes of C₂—H and C_{4,5}—H on the imidazole ring of [C₂mim][NTf₂]. It can be observed that IR absorbance of C—H stretching (3220–2800 cm⁻¹) is enhanced by the existence of PNIPAM, and a small shift toward lower wavenumber can be noted where bands are assigned to C=O groups, which implies that there is weak interaction between [C₂mim][NTf₂] and PNIPAM.

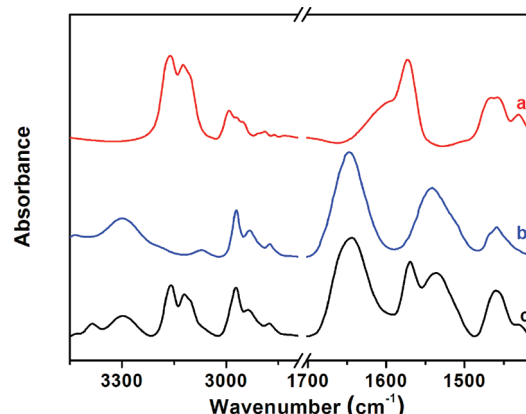


Figure 3. FTIR spectra of pure ionic liquid [C₂mim][NTf₂] (a), of PNIPAM (b), and of 10 wt % PNIPAM/[C₂mim][NTf₂] gel (c).

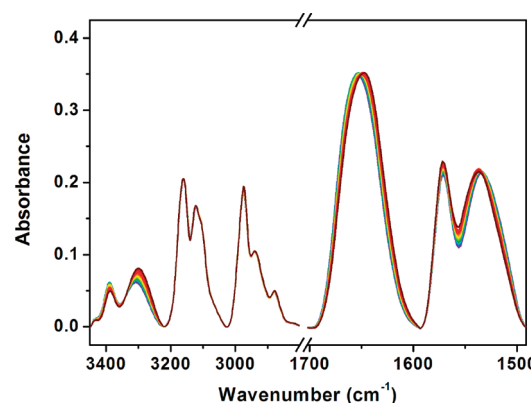


Figure 4. Temperature-dependent FTIR spectra of 10 wt % PNIPAM/[C₂mim][NTf₂] during cooling from 50 to 25 °C.

The whole gelation process of PNIPAM was *in situ* monitored by FTIR spectroscopy upon cooling from 50 to 25 °C (Figure 4). Three spectral regions are mainly focused in this Article (Figure 5): the N—H stretching band of PNIPAM (3450–3220 cm⁻¹), the C—H stretching band of imidazole ring (3220–3025 cm⁻¹), and the amide I (C=O hydrogen bonding) (1702–1592 cm⁻¹). By analyzing these three regions, information on the molecular motion of chemical groups during gelation could be provided. For clarity, the second derivative spectra of the three regions at 50, 37, and 25 °C are also shown to enhance the spectral resolution to investigate further the slight variation induced by phase separation (Figure 6).

In Figure 5a, the spectra of the N—H stretching region are shown. Three obvious bands centered around 3435, 3387, and 3299 cm⁻¹ could be observed as well as in Figure 6a. The bands of 3387 and 3299 cm⁻¹, which are assigned to the hydrogen bonds of N—H···IL and N—H···O=C, respectively, both shift to lower wavenumbers during cooling, resulting from the enhancement of interaction in the system during gelation. The intensity of the 3387 cm⁻¹ bands shows a continuous decrease during cooling, whereas the intensity of the 3299 cm⁻¹ band increases continuously; this evidence confirmed that N—H groups have preferential interaction with the C=O groups during gelation. Moreover, it is noted that the 3435 cm⁻¹ band that originated from free N—H stretching vibrations³⁸ experiences a slight decrease with the decrease in temperature.

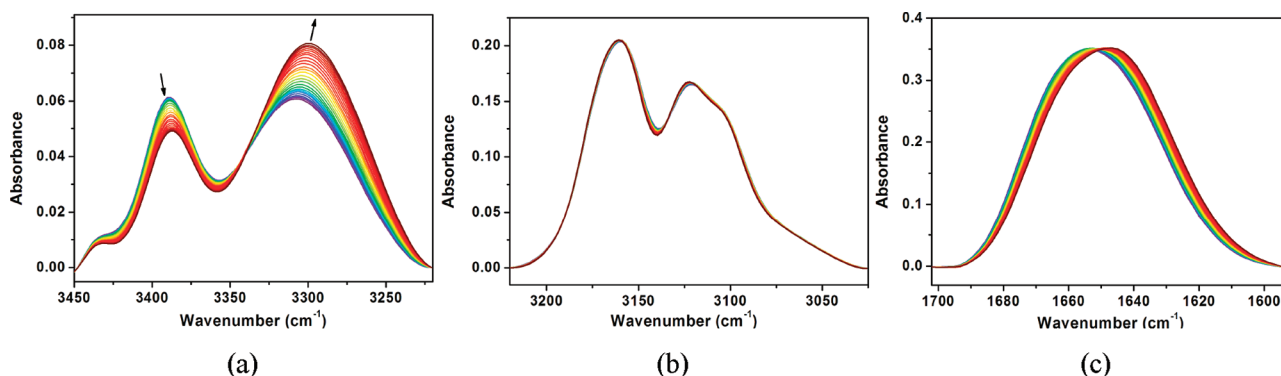


Figure 5. Temperature-dependent FTIR spectra of PNIPAM in $[C_2\text{mim}][\text{NTf}_2]$ (10 wt %) in the $\nu(\text{N}-\text{H})$ region (a), $\nu(\text{C}-\text{H})$ region of imidazole ring (b), and $\nu(\text{C}=\text{O})$ region (c) during cooling from 50 to 25 °C.

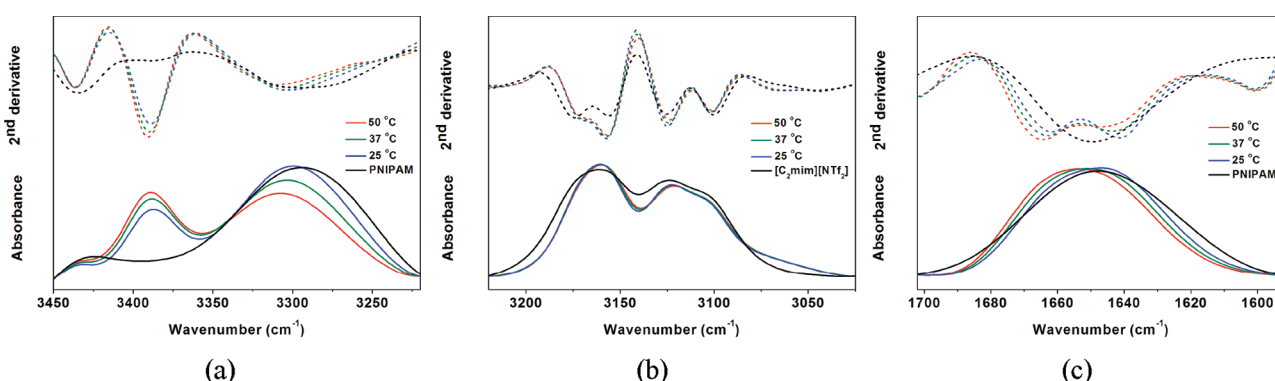


Figure 6. FTIR and corresponding second-derivative spectra of $\nu(\text{N}-\text{H})$ region (a), $\nu(\text{C}-\text{H})$ region of imidazole ring (b), and $\nu(\text{C}=\text{O})$ region (c) of sample with 10 wt % PNIPAM at different temperatures (50, 37, and 25 °C). Black lines represent the neat PNIPAM (a,c) and $[C_2\text{mim}][\text{NTf}_2]$ (b) at 25 °C, respectively.

This might be ascribed to the limited motion space for polymer chains in gelation progress. Compared with the neat PNIPAM, it is also noted that the hydrogen bonds of $\text{N}-\text{H}\cdots\text{O}=\text{C}$ at three different temperatures all shift to higher wavenumbers in Figure 6a, which is in accord with our supposition that the existence of ILs leads to the weakness of the interaction between polymer chains and the formation of new interaction between polymer and ILs.

All spectra of N–H stretching region could be curve-fitted simultaneously over the whole temperature range. The decomposed spectra at 50, 40, 30, and 25 °C are given as examples in Figure 7a. In accordance with the second derivative results, three bands were found. To describe quantitatively the phase transition processes during cooling, integral areas of two bands around 3387 and 3299 cm⁻¹ are analyzed in Figure 7b, in which a different changing trend between the hydrogen bonds of $\text{N}-\text{H}\cdots\text{IL}$ and $\text{N}-\text{H}\cdots\text{O}=\text{C}$ ³⁸ is found. From focus in Figure 7b-1, the peak area of hydrogen bond of $\text{N}-\text{H}\cdots\text{IL}$ goes through a slight decrease at the beginning of cooling, then deceases sharply around T_{gel} , and has a gentle change ultimately. Relatively, the integral area of hydrogen bond of $\text{N}-\text{H}\cdots\text{O}=\text{C}$ experiences a continuous increase with no obvious stage change, which is observed in Figure 7b-2. Therefore, the response to temperature variation for the $\text{N}-\text{H}\cdots\text{IL}$ hydrogen bond is different from that for the $\text{N}-\text{H}\cdots\text{O}=\text{C}$ hydrogen bond; the latter is more sensitive.

Bands in the range of 3220–3025 cm⁻¹ originated from C–H stretching vibrations of the imidazole ring are shown in Figure 5b,

where slight differences can be noted in 1DIR but be valued for the investigation on the ion environment. Four bands were found, together with a small shift toward lower wavenumber compared with neat $[C_2\text{mim}][\text{NTf}_2]$, especially for the band at highest wavenumber, which is illuminated in the second-derivative spectra of Figure 6b. As is well known, the imidazolium C–H stretching region may be described by two doublets (four bands); one doublet at the lower frequencies is attributed to the C_2 –H stretching modes, and the other at the higher frequencies is assigned to the coupled C_4 –H and C_5 –H stretching modes.⁵ Previous studies have shown that the shifts of C–H bands are closely related to changes in the liquid structure and solvation states,^{5,7,9,39,40} and thus our observations suggest that the addition of PNIPAM molecules may adjust the cation–anion clusters via the interactions between cation and PNIPAM and anion and PNIPAM. A further explanation of these phenomena in the region will be discussed in the following PCMW and 2D analysis.

Figure 5c shows the temperature dependence of the absorption bands of the $\text{C}=\text{O}$ groups in 10 wt % PNIPAM/ $[C_2\text{mim}][\text{NTf}_2]$ (50–25 °C) during gelation, where spectral changes can be noted, but from the 1D FTIR spectra, we cannot make sure that the changes arise from the peak shift or the component change of an overlapped band. For clarity, the second-derivative spectra of the amide I region are shown in Figure 6c, where two obvious bands centered around 1665 and 1640 cm⁻¹ could be observed during the whole gelation process. Therefore, it is

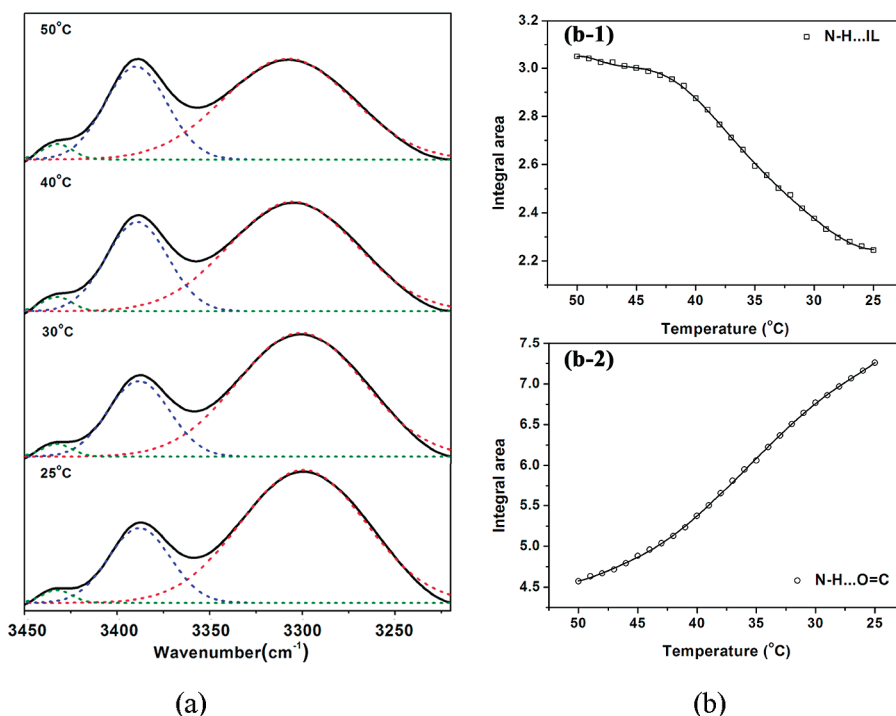


Figure 7. Deconvoluted infrared spectrum (a) of the N–H stretching region of PNIPAM in $[C_2\text{mim}][\text{NTf}_2]$ (10 wt %) at different temperatures (50, 40, 30, and 25 °C). Temperature-dependent integral area (b) of 3387 cm^{-1} band (b-1) and 3299 cm^{-1} band (b-2) during cooling process.

considered that the spectral changes of the $\nu(\text{C=O})$ region are due to the increase in the intensity of the 1640 cm^{-1} band, together with the decrease in the intensity of the 1665 cm^{-1} band. As the bands of 1640 and 1665 cm^{-1} are assigned to the hydrogen bonds of $\text{C=O}\cdots\text{H-N}$ and oxygen atoms of C=O groups H-bonded with C–H groups of imidazole ring, respectively, this evidence confirms that when PNIPAM chains go through the sol-to-gel transition their C=O groups preferentially interact with their N–H groups compared with C–H groups of imidazole ring. Moreover, for neat PNIPAM, the amide I band arises only from the C=O hydrogen bonded to N–H, whereas the amide I band of PNIPAM/ $[C_2\text{mim}][\text{NTf}_2]$ continuously splits into two bands at 1665 and 1640 cm^{-1} , which is due to the two different kinds of hydrogen bonds in the sample. It indicates that the relative transformation between those two kinds of hydrogen bonds probably results in the sol–gel transition during cooling.

3.3. Perturbation Correlation Moving Window Analysis. To ascertain the gelation of PNIPAM in $[C_2\text{mim}][\text{NTf}_2]$ more accurately, we performed a PCMW analysis. The PCMW method, which was proposed by Thomas³³ and later improved by Morita³⁴ in 2006, can correlate the external perturbations directly with changes in the peaks; therefore, it is not only used to determine the critical transition points of the samples but also used to monitor the complicated spectral variations along the perturbation direction, particularly weak phase transitions that are difficult to observe by other methods.

Two types of spectra (synchronous and asynchronous) can be generated by PCMW. The rules of PCMW are as follows: with the increment of perturbation, positive synchronous correlation stands for the increase in spectral intensities, whereas negative synchronous correlation stands for the decrease in spectral intensities; positive asynchronous correlation corresponds to a convex

spectral intensity variation, whereas negative asynchronous correlation corresponds to a concave variation.³⁴ In this Article, only the synchronous spectra of PCMW are presented in Figure 8 for the determination of PNIPAM/ $[C_2\text{mim}][\text{NTf}_2]$ during cooling.

The T_{gel} is hardly obtained from the temperature-dependent integral area curves, which are not the traditional Boltzmann-fitted variations,^{35,41} but according to Morita's PCMW rule,³⁴ PCMW synchronous spectra are very helpful to find transition points. Therefore, for $\text{C=O}\cdots\text{H-N}$ and $\text{N-H}\cdots\text{IL}$ hydrogen bonds, T_{gel} is around $36\text{ }^\circ\text{C}$, and for $\text{C}_{2,4,5}\text{-H}\cdots\text{O=C}$ hydrogen bonds, T_{gel} is around $37\text{ }^\circ\text{C}$. These show that $\text{C}_{2,4,5}\text{-H}\cdots\text{O=C}$ hydrogen bonds have an earlier response during gelation process, namely, the strength of hydrogen bonds between PNIPAM and anions is weaker than that between PNIPAM and cations.

It is worth noting that the change of the ions environment can also be determined in PCMW synchronous map during the gelation process. In Figure 8, two doublets (four bands) are mainly observed in the $\nu(\text{C–H})$ region of $3220\text{--}3025\text{ cm}^{-1}$ as well as the second derivate spectra in Figure 6b; that is, the one at the lower frequencies is assigned to the $\text{C}_2\text{-H}$ stretching vibrations, whereas the other at the higher frequencies is attributed to the $\text{C}_{4,5}\text{-H}$ stretching vibrations. The splitting of the bands in doublets was ascribed to the existence in the bulk phase of isolated pairs with stronger hydrogen bonds to the counteranion in addition to associated pairs with weaker hydrogen bonds.⁵ For a system involving binary mixture or multi-element, the associated species may be larger ion clusters (or ion pairs), and the isolated species may mean the dissociation into smaller ion clusters (or free ions).^{9,10}

The associated species may be completely H-bonded via $\text{C}_2\text{-H}$ and $\text{C}_{4,5}\text{-H}$, whereas the isolated species are not fully H-bonded. Because of the anticooperative charge transfer within

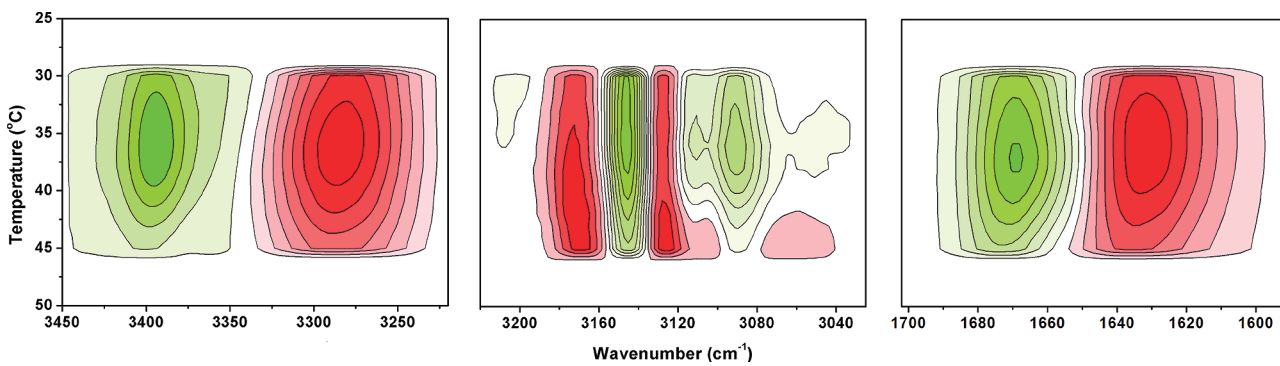


Figure 8. PCMW synchronous of PNIPAM/[C₂mim][NTf₂] generated from all spectra between 50 and 25 °C. Here warm colors (red) are defined as positive intensities, whereas cool colors (green) are defined as negative intensities.

the imidazolium ring, such hydrogen bonds in associated species are weaker than those in isolated species.⁵ Obviously, with the reduction of temperature, the intensity of bands at 3172 and 3126 cm⁻¹ increase, whereas the intensity of 3145 and 3091 cm⁻¹ bands decreases, which is hard to obtain from conventional 1DIR analysis but can be observed in PCMW synchronous spectra. Because the 3172 and 3126 cm⁻¹ bands and the 3145 and 3091 cm⁻¹ bands are assigned to the hydrogen bonds of associated species and isolated species,^{5,10} respectively, this evidence confirms that the ion environment experiences the change of the relative components between the associated and isolated species. In the gelation process, the increase in associated species is possibly due to the aggregation of the isolated ones and liberation of ions H-bonded with polymer. Additionally, it is worth noting that the transition temperatures of associated-related bands are apparently higher than those of isolated-related bands during cooling, indicating that associated species may have an earlier response than isolated species in gelation, which can also be confirmed by later 2Dcos analysis.

3.4. Two-Dimensional Correlation Analysis. In 2D correlation analysis, two types of correlation maps including synchronous and asynchronous spectra are obtained from a series of dynamic spectra, which are characterized by two independent “wavenumber” axes (ν_1, ν_2) and a correlation intensity axis. The correlation intensities in the synchronous and asynchronous maps reflect the relative degree of in-phase and out-of phase responses, respectively.

On the 2D synchronous maps, peaks are symmetric with respect to the diagonal line in the correlation map. Peaks appearing along the diagonal are called “autopeaks”, which are always positive, indicating that the peak at the same wavenumber changes greatly under the external perturbation. The off-diagonal peaks ($\Phi(\nu_1, \nu_2)$) are cross peaks, which may be positive or negative. The positive cross-peaks ($\Phi(\nu_1, \nu_2)$) demonstrate that both peaks ν_1 and ν_2 change in the same direction (both increase or decrease) under the perturbation, whereas negative cross-peaks infer that the intensities of peaks ν_1 and ν_2 change in opposite directions. (One increases, whereas the other one decreases.)

In 2D asynchronous spectra, there is no autopeak but only off-diagonal cross-peaks, which can be either positive or negative. According to Noda’s rule, if the rcross-peak (ν_1, ν_2 , and assume $\nu_1 > \nu_2$) in the synchronous and asynchronous maps has the same sign (both positive or both negative), then the change of peak ν_1 may occur prior to that of ν_2 and vice versa. Hence,

Table 1. Tentative Band Assignments of PNIPAM/[C₂mim][NTf₂] (10 wt %) during Gel Formation Process

wavenumber (cm ⁻¹)	assignments
3435	ν (free N–H) in PNIPAM
3387	ν (N–H...[NTf ₂] ⁻)
3299	ν (N–H...O=C)
3172	ν (C _{4,5} –H) in hydrogen bonds of associated species in [C ₂ mim][NTf ₂]
3145	ν (C _{4,5} –H) in hydrogen bonds of isolated species in [C ₂ mim][NTf ₂]
3126	ν (C ₂ –H) in hydrogen bonds of associated species of [C ₂ mim][NTf ₂]
3091	ν (C ₂ –H) in hydrogen bonds of isolated species of [C ₂ mim][NTf ₂]
2991	ν_{as} (CH ₃) in imidazolium ring of [C ₂ mim][NTf ₂]
2968	ν_{as} (CH ₃) in side chains of PNIPAM
2923	ν_{as} (CH ₂) in main chains of PNIPAM
2870	ν_s (CH ₃) in side chains of PNIPAM
1670	ν (C=O...C _{4,5} –H)
1650	ν (C=O...C ₂ –H)
1631	ν (C=O...H–N)

combined with synchronous and asynchronous spectra, some useful information about the temporal sequence of events can be obtained. For the convenience of discussion, spectral assignments of the all bands for 2Dcos analysis have been presented in Table 1.

3.4.1. Variation of Ion Environment during Cooling. Two-dimensional synchronous and asynchronous spectra in the region of 3220–3025 cm⁻¹ of the cooling process are depicted in Figure 9, from which we can get an insight into changes happening to the cations and anions during gelation.

In the synchronous maps of Figure 9a, autopeaks mainly appear at 3172, 3145, 3126, and 3091 cm⁻¹, indicating the intensities of these bands change greatly under the perturbation of temperature. In the synchronous maps of Figure 9b, in addition to the four bands, a new band at ~3060 cm⁻¹ attributed from amide B of PNIPAM³⁷ could be identified, which may be hard to observe because of the overlapping of peaks in 1DIR. As focused on the ion environment, the former four bands related to the ionic liquid attract more of our attention, and thus we concentrate on analyzing these bands hereafter.

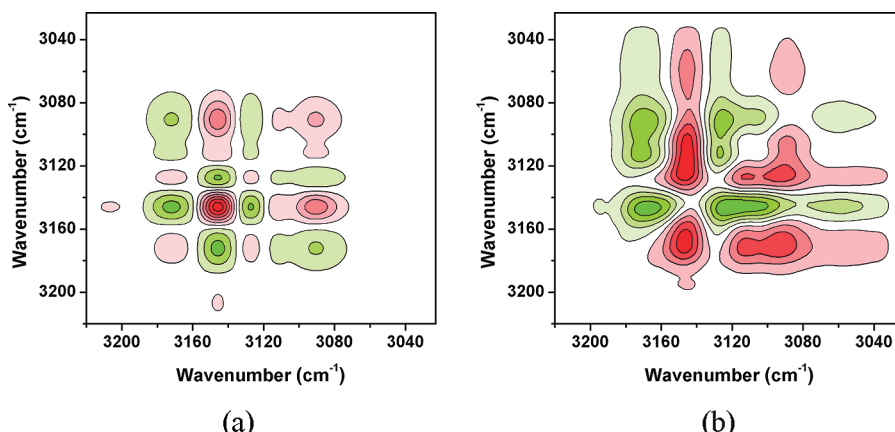


Figure 9. Two-dimensional synchronous and asynchronous spectra in $\nu(\text{C}-\text{H})$ region of $3220-3025 \text{ cm}^{-1}$ during cooling obtained from all spectra between 50 and 25 °C. Warm colors (red) refer to positive intensities, whereas cold colors (green) refer to negative intensities.

To make their transformation relationships clear, we then calculate cross peaks on synchronous and asynchronous maps by 2DIR. A simplified method for determination of sequence order has been previously described. Results were gained according to Noda's rule,^{31,32} from which we could obtain the final specific order of these four different bands as follows (\rightarrow means prior to or earlier than): $3126 \rightarrow 3172 \rightarrow 3145 \rightarrow 3091 \text{ cm}^{-1}$, that is, $\nu(\text{C}_2-\text{H})$ in hydrogen bonds associated species $\rightarrow \nu(\text{C}_{4,5}-\text{H})$ in hydrogen bonds of associated species $\rightarrow \nu(\text{C}_{4,5}-\text{H})$ in hydrogen bonds of isolated species $\rightarrow \nu(\text{C}_2-\text{H})$ in hydrogen bonds of isolated species. In light of the transition sequence, it could be summarized that the associated species have the thermal response prior to the isolated species, which is in accordance with the PCMW results. Namely, as the temperature decreases, the molecular structures in $[\text{C}_2\text{mim}][\text{NTf}_2]$ begin to adjust with the associated species constructed; then, more isolated ones are released, which are H-bonded with polymer at higher temperature. In associated species, the prior appearance of the hydrogen bonds via C_2-H is mainly ascribed to the acidity and the more stable positions. It is well known that the charge of carbon C_2 of the imidazolium ring is positive owing to the electron deficit in the $\text{C}=\text{N}$ bond, whereas C_4 and C_5 are practically neutral, which results in the acidity of the hydrogen atoms,^{4,8,42} and thus the interaction of C_2-H with anion is stronger than that of $\text{C}_{4,5}-\text{H}$ with anion. In addition, conformers with the anion in front of the C_2-H bond and on top of C_2 of the imidazolium ring are energetically preferred, whereas in-plane positions near C_4-H and C_5-H are markedly less stable.^{4,8} The sequential order given by 2DIR analysis can be explained that the formation of associated species is favored via C_2-H bonded with $[\text{NTf}_2]^-$ for enthalpic reasons, then the weak hydrogen bonds via $\text{C}_{4,5}-\text{H}$ are constructed. The lower the temperature, the greater the quantity of associated species, and thus the hydrogen bonds between isolated species and polymer will be destroyed. Because the hydrogen bonds formed between $\text{C}_{4,5}-\text{H}$ and polymer are much weaker than those via C_2-H , $\text{C}_{4,5}-\text{H}$ attributed to the isolated species will remove such a hydrogen bond earlier to participate in the associated species formation, with the final immobilization of the associated ones by polymer network, which will be discussed in a later part.

In the ion environment, the relative contribution of the isolated and associated components is obviously temperature-dependent; that is, the construction of associated ones can

favorably compete before the motion of polymeric groups with temperature decreasing, which is the possible driving force in the gelation process. It is in accordance with the PCMW results that the transition temperature of the associated components is higher than that of PNIPAM, which means the response to the thermal perturbation for ion environment is more sensitive.

3.4.2. Group Motions of PNIPAM in the Gelation Process. With the change of the ion environment described above, the microstate changes of the polymeric groups were believed to occur during the gelation process. Figure 10 is the synchronous and asynchronous maps calculated by 2Dshige software in the regions of $\nu(\text{N}-\text{H})$, $\nu(\text{C}-\text{H})$, and $\nu(\text{C}=\text{O})$ originated from PNIPAM. Correlated 1DIR of these spectra ranges are already shown in Figure 4, where the $\nu(\text{N}-\text{H})$ and $\nu(\text{C}=\text{O})$ regions have significant changes, whereas the region of $\nu(\text{C}-\text{H})$ scarcely shows variations. It is revealed that the group motions of PNIPAM turn up following the change of relative contribution of the isolated and associated components in $[\text{C}_2\text{mim}][\text{NTf}_2]$ previously mentioned. Similarly, 2DIR is applied to deduce the sequential order of the group motions of PNIPAM, and the final results have been obtained, which can be extracted as follows: $1670 \rightarrow 1650 \rightarrow 1631$ and $3299 \rightarrow 3387 \rightarrow 2968 \rightarrow 2923 \text{ cm}^{-1}$. Without considering the different vibrational modes, the sequence can be described as: $\nu(\text{C}=\text{O})$ on the side chains $\rightarrow \nu(\text{N}-\text{H})$ on the side chains $\rightarrow \nu_{\text{as}}(\text{CH}_3)$ on the side chains $\rightarrow \nu_{\text{as}}(\text{CH}_2)$ on the main chains. This sequence order can be interpreted at the following aspects:

(1). $\nu(\text{N}-\text{H})$ Region of $3450-3220 \text{ cm}^{-1}$. In Figure 10a, the synchronous data imply that bands at 3299 and 3387 cm^{-1} are both susceptible to temperature reduction. As seen in the asynchronous spectrum (Figure 10b), several cross peaks appear, which suggests the asynchronism of responses given by corresponding molecular vibrations toward the thermal perturbation. However, some of them are fake peaks produced by baseline variations or affected by the shift of bands, which can be excluded by comparison with 1DIR. In particular, it is notable that the 3435 cm^{-1} band assigned to free $\text{N}-\text{H}$ groups vibrations, which could be seen in 1DIR, disappears in the 2Dcos maps, probably because the response of them is negligible compared with the bonded $\text{N}-\text{H}$ groups.

According to our previous expectation, we focus on the bonded ones located at around 3299 and 3387 cm^{-1} . The finally discerned transform order ($3299 \rightarrow 3387 \text{ cm}^{-1}$) reveals that the

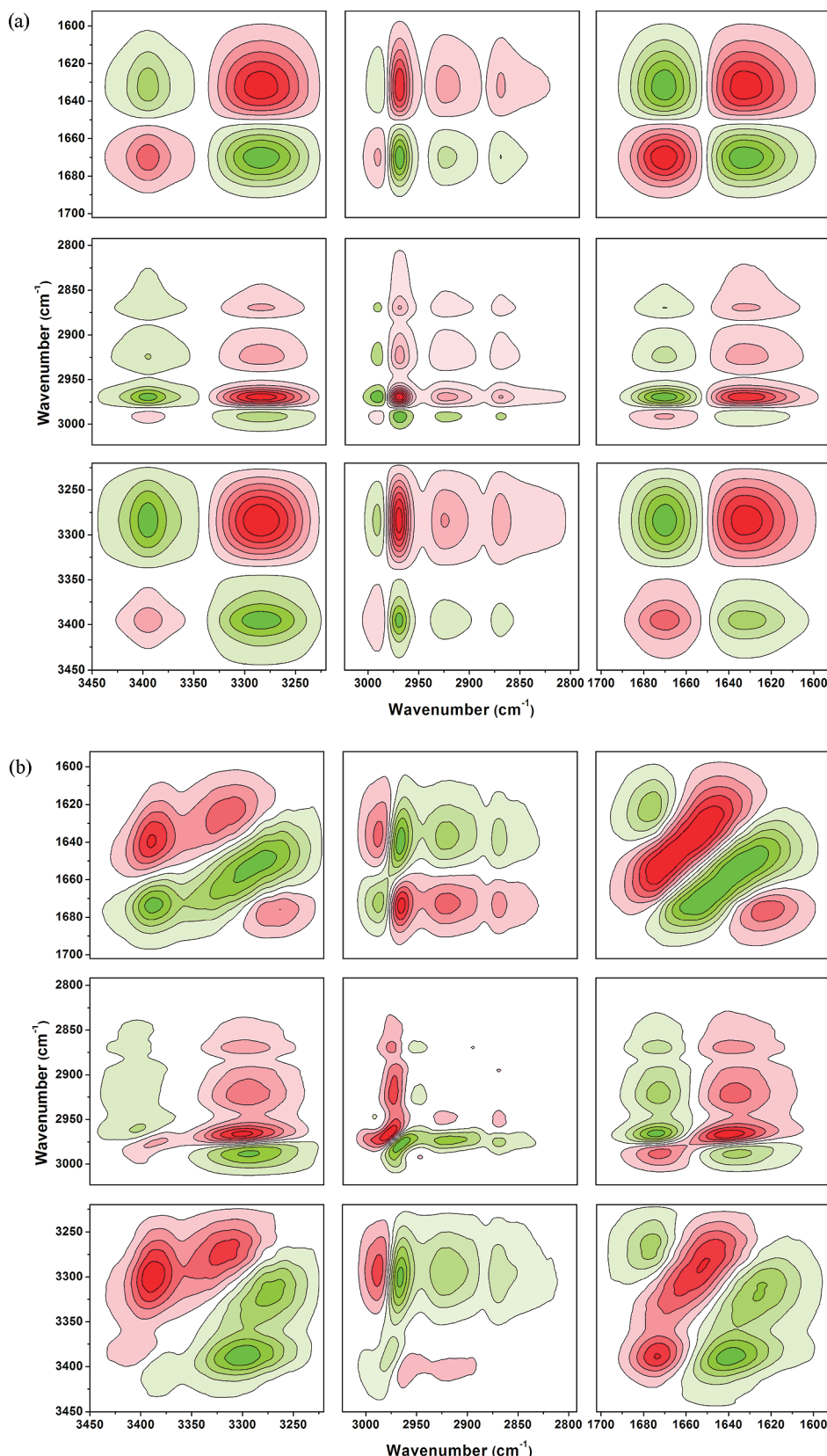


Figure 10. Two-dimensional synchronous (a) and asynchronous (b) spectra in $\nu(\text{N}-\text{H})$, $\nu(\text{C}-\text{H})$, and $\nu(\text{C}=\text{O})$ regions of PNIPAM in $[\text{C}_2\text{mim}][\text{NTf}_2]$ during gelation generated from all spectra between 50 and 25 °C. Warm colors (red) refer to positive intensities, whereas cold colors (green) refer to negative intensities.

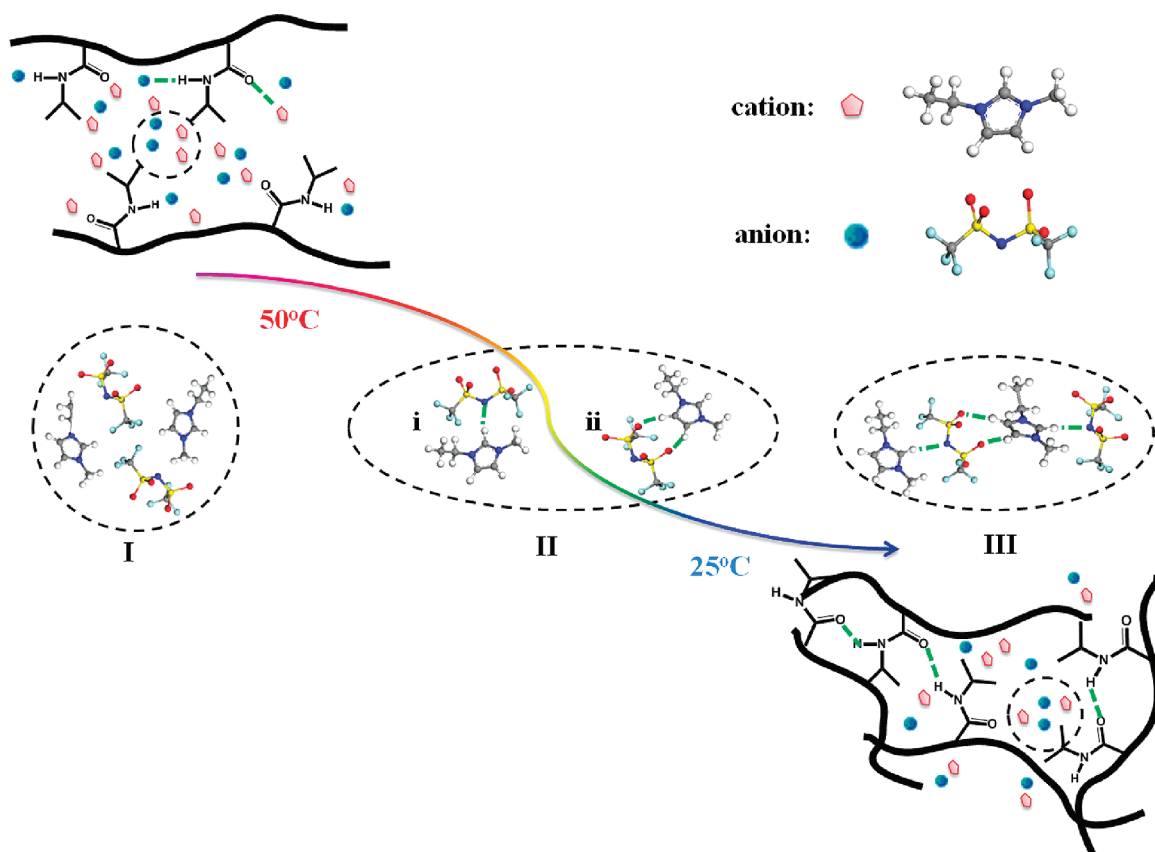


Figure 11. Schematic illustration of the gelation microdynamic mechanism of PNIPAM gelation in $[C_2\text{mim}][\text{NTf}_2]$ during cooling. The pink five-angle rings represent the cations of $[C_2\text{mim}][\text{NTf}_2]$, and the blue balls represent the anions of the IL. Also, the corresponding structures of anion and cation are illustrated.

N–H groups have preferential interaction with C=O groups of the other side chains with the anions of ionic liquid, leading to the final formation of the network structure among polymer chains.

(2). $\nu(C-H)$ Region of 3023–2792 cm^{-1} . In the synchronous map of Figure 10a, autopeaks exist in four main bands centered at 2991, 2968, 2923, and 2870 cm^{-1} , indicating that these bands change greatly with the temperature variation. According to the assignments in Table 1, the 2991 cm^{-1} band arises from the CH₃ groups of the imidazolium ring,⁴³ whereas the other three bands located at lower wavenumbers are assigned to $\nu_{as}(\text{CH}_3)$, $\nu_{as}(\text{CH}_2)$, and $\nu_s(\text{CH}_2)$ of PNIPAM, where we pay more attention. The peak at (2968, 2923) cm^{-1} in Figure 10, positive in both the synchronous and asynchronous maps, reveals that the vibration of $\nu_{as}(\text{CH}_3)$ changes earlier than that of $\nu_{as}(\text{CH}_2)$, supporting the conclusion that the motion of CH side groups occurs before those groups on the backbone of PNIPAM during the polymer network formation.

(3). $\nu(C=O)$ Region of 1702–1592 cm^{-1} . For C=O related vibrations, the sequence can be extracted as follows: 1670 → 1650 → 1631 cm^{-1} , that is, $\nu(C=O \cdots C_{4,5}-H) \rightarrow \nu(C=O \cdots C_2-H) \rightarrow \nu(C=O \cdots H-N)$. Namely, hydrogen bonds between C=O groups and cations will be broken as gel formation; then, new interactions between C=O and N–H groups will be constructed. The interaction of C_{4,5}-H with C=O is weaker than that of C₂-H with C=O;¹⁰ that is, the weaker the interactions are, the higher the wavenumber of $\nu(C=O)$ will be. Therefore, the peak centered at 1670 cm^{-1} could be assigned to hydrogen bonds of C_{4,5}-H interacting with

C=O, and that at 1650 cm^{-1} could be assigned to C₂-H with C=O hydrogen bonds. Because of the weaker H bonds via C_{4,5}, C=O groups will remove such a hydrogen bond earlier as a result of the change of ion environment, which is confirmed in the 3220–3025 cm^{-1} region mentioned above. Then, free C=O groups will prefer to interact with N–H groups nearby, followed by the dissociation of interaction between N–H groups and anions.

On the basis of the above analysis during cooling, we could clearly understand the microstate leveled interaction between ion environment and polymer chains in the gelation process. For a more intuitionistic understanding of the microdynamic mechanism, all proven and assigned structures are illustrated in Figure 11. The isolated and associated components of $[C_2\text{mim}][\text{NTf}_2]$ are represented by I, II, and III, respectively, where the isolated species mean small ion clusters (or free ions) and the associated species may be the aggregation of isolated species (type I presents the free ions; type II presents the ion pairs H-bonded via C₂-H (i) and C_{4,5}-H (ii); type III presents the associated species fully H-bonded with neighboring anions via C₂-H and C_{4,5}-H).^{5,44}

At higher temperature above T_{gel} , the ions mainly exist in the form of I or II, with some of them interacting with the C=O and N–H groups of polymer, which results in the extension of polymer chain in the IL. As the temperature decreases, the isolated species begin to interact with each other and then aggregate to the associated species; (ii) is not as stable as (i), so the structure (i) appears earlier. Upon the driving force of the

alteration of the isolated and associated components in system, the $\text{C}=\text{O}\cdots\text{C}_{4,5}-\text{H}$ hydrogen bond is broken prior to hydrogen bond of $\text{C}=\text{O}\cdots\text{C}_2-\text{H}$ as temperature decreases to above T_{gel} , after that $\text{N}-\text{H}\cdots\text{O}=\text{C}$ hydrogen bonds are constructed. Furthermore, the formation of preferential H bonds in $\text{N}-\text{H}\cdots\text{O}=\text{C}$ near T_{gel} destroy the interaction between $\text{N}-\text{H}$ group and anions, leading to a continuous shrinkage of the polymer chain from the pendent alkyl groups to the backbone. Finally, the gel formation appears with the immobilization of the associated species in polymer network. Possibly, the construction of associated species related to solvation in ILs is the driving force on the sol-to-gel transition of PNIPAM,^{5,27,36} which, meanwhile, is actually a desolvation process upon the variation of ion environment.

4. CONCLUSIONS

FTIR spectroscopy in combination with 2Dcos and PCMW technique is employed for the first time to illustrate the gelation microdynamic mechanism of PNIPAM in a ionic liquid [$\text{C}_2\text{mim}]^+[\text{NTf}_2]^-$] cooling from 50 to 25 °C. We focus mainly on three regions ($3450\text{--}3220\text{ cm}^{-1}$ for $\nu(\text{N}-\text{H})$, $3220\text{--}3025\text{ cm}^{-1}$ for $\nu(\text{C}-\text{H})$ of imidazole ring, and $1702\text{--}1592\text{ cm}^{-1}$ for $\nu(\text{C}=\text{O})$) in this Article.

Appreciable changes in band frequencies and shapes can be observed for the $\nu(\text{N}-\text{H})$ and $\nu(\text{C}=\text{O})$ regions, indicating the formation of a new interaction between the ionic liquids and PNIPAM and the transformation of interior interaction between polymer chains during gelation. In $3220\text{--}3025\text{ cm}^{-1}$, although slight changes can be noted in 1DIR, the region is valued for the investigation of the ion environment. 2Dcos results suggest that the variation of the ion environment takes place with the relative change of the isolated (free ions or smaller ion pairs) and associated (larger ion clusters) components of $[\text{C}_2\text{mim}]^+[\text{NTf}_2]^-$. The construction of associated species related to solvation in ILs is the possible driving force on the sol-to-gel transition of PNIPAM.

PCMW easily determined the transition temperature, and 2Dcos analysis indicated the microdynamic mechanism during gelation. Upon cooling, following the change of ion environment, the side chains of PNIPAM experience a changing process from dissociation of the interaction with ionic liquid to formation of $\text{N}-\text{H}\cdots\text{O}=\text{C}$ hydrogen bonding, where the $\text{C}=\text{O}$ groups remove the weaker hydrogen bonds via $\text{C}_{4,5}-\text{H}$ earlier than that via C_2-H . Moreover, the motion of side chains occurs before that of the PNIPAM backbone, leading to the shrinkage of polymer from the side chains to backbone together with forming the polymer network. Finally, the immobilization of the associated species in the polymer chains network results in the opaque gel formation, which, meanwhile, is actually a desolvation process upon the variation of ion environment.

■ AUTHOR INFORMATION

Corresponding Author

*E-mail: peiyiwu@fudan.edu.cn.

■ ACKNOWLEDGMENT

We gratefully acknowledge the financial support from National Science Foundation of China (NSFC) (20934002, S1073043) and the National Basic Research Program of China (no. 2009CB930000).

■ REFERENCES

- Welton, T. *Chem. Rev.* **1999**, *99*, 2071–2084.
- Smiglak, M.; Metlen, A.; Rogers, R. D. *Acc. Chem. Res.* **2007**, *40*, 1182–1192.
- Lu, J.; Yan, F.; Texter, J. *Prog. Polym. Sci.* **2009**, *34*, 431–448.
- Weingartner, H. *Angew. Chem., Int. Ed.* **2008**, *47*, 654–670.
- Köddermann, T.; Wertz, C.; Heintz, A.; Ludwig, R. *ChemPhysChem* **2006**, *7*, 1944–1949.
- Tsuzuki, S.; Tokuda, H.; Mikami, M. *Phys. Chem. Chem. Phys.* **2007**, *9*, 4780–4784.
- Fumino, K.; Wulf, A.; Ludwig, R. *Angew. Chem., Int. Ed.* **2008**, *47*, 8731–8734.
- Wulf, A.; Fumino, K.; Ludwig, R. *Angew. Chem., Int. Ed.* **2010**, *49*, 449–453.
- Yokozeki, A.; Kasprzak, D. J.; Shiflett, M. B. *Phys. Chem. Chem. Phys.* **2007**, *9*, 5018–5026.
- Jiang, J. C.; Li, S. C.; Shih, P. M.; Hung, T. C.; Chang, S. C.; Lin, S. H.; Chang, H. C. *J. Phys. Chem. B* **2011**, *115*, 883–888.
- Hou, J.; Zhang, Z.; Madsen, L. A. *J. Phys. Chem. B* **2011**, *115*, 4576–4582.
- Kubisa, P. *Prog. Polym. Sci.* **2009**, *34*, 1333–1347.
- Ueki, T.; Watanabe, M. *Macromolecules* **2008**, *41*, 3739–3749.
- Susan, M. A. B. H.; Kaneko, T.; Noda, A.; Watanabe, M. *J. Am. Chem. Soc.* **2005**, *127*, 4976–4983.
- Fuller, J.; Breda, A.; Carlin, R. *J. Electrochem. Soc.* **1997**, *144*, L67–L70.
- Yeon, S. H.; Kim, K. S.; Choi, S.; Cha, J. H.; Lee, H. *J. Phys. Chem. B* **2005**, *109*, 17928–17935.
- Singh, B.; Sekhon, S. *J. Phys. Chem. B* **2005**, *109*, 16539–16543.
- Harnet, J. M.; Hoagland, D. A. *J. Phys. Chem. B* **2010**, *114*, 3411–3418.
- Klingshirn, M. A.; Spear, S. K.; Subramanian, R.; Holbrey, J. D.; Huddleston, J. G.; Rogers, R. D. *Chem. Mater.* **2004**, *16*, 3091–3097.
- Kawauchi, T.; Kumaki, J.; Okoshi, K.; Yashima, E. *Macromolecules* **2005**, *38*, 9155–9160.
- Ueki, T.; Watanabe, M. *Chem. Lett.* **2006**, *35*, 964–965.
- Ueki, T.; Watanabe, M. *Langmuir* **2007**, *23*, 988–990.
- Kodama, K.; Nanashima, H.; Ueki, T.; Kokubo, H.; Watanabe, M. *Langmuir* **2009**, *25*, 3820–3824.
- He, Y.; Lodge, T. P. *Chem. Commun.* **2007**, 2732–2734.
- He, Y.; Lodge, T. P. *Macromolecules* **2008**, *41*, 167–174.
- He, Y.; Boswell, P. G.; Höglmann, P.; Lodge, T. P. *J. Phys. Chem. B* **2007**, *111*, 4645–4652.
- Fujii, K.; Ueki, T.; Niituma, K.; Matsunaga, T.; Watanabe, M.; Shibayama, M. *Polymer* **2011**, *52*, 1589–1595.
- Ding, Y.; Ye, X.; Zhang, G. *Macromolecules* **2005**, *38*, 904–908.
- Zhou, K.; Lu, Y.; Li, J.; Shen, L.; Zhang, G.; Xie, Z.; Wu, C. *Macromolecules* **2008**, *41*, 8927–8931.
- Sun, B.; Lin, Y.; Wu, P.; Siesler, H. W. *Macromolecules* **2008**, *41*, 1512–1520.
- Noda, I. *J. Am. Chem. Soc.* **1989**, *111*, 8116–8118.
- Noda, I. *J. Mol. Struct.* **2010**, *974*, 3–24.
- Thomas, M.; Richardson, H. H. *Vib. Spectrosc.* **2000**, *24*, 137–146.
- Morita, S.; Shinzawa, H.; Noda, I.; Ozaki, Y. *Appl. Spectrosc.* **2006**, *60*, 398–406.
- Sun, S.; Hu, J.; Tang, H.; Wu, P. *J. Phys. Chem. B* **2010**, *114*, 9761–9770.
- Winterton, N. *J. Mat. Chem.* **2006**, *16*, 4281–4293.
- Köddermann, T.; Ludwig, R. *Phys. Chem. Chem. Phys.* **2004**, *6*, 1867–1873.
- Sun, B.; Lin, Y.; Wu, P. *Appl. Spectrosc.* **2007**, *61*, 765–771.
- Chang, H. C.; Jiang, J. C.; Su, J. C.; Chang, C. Y.; Lin, S. H. *J. Phys. Chem. A* **2007**, *111*, 9201–9206.
- Chang, H. C.; Jiang, J. C.; Chang, C. Y.; Su, J. C.; Hung, C. H.; Liou, Y. C.; Lin, S. H. *J. Phys. Chem. B* **2008**, *112*, 4351–4356.
- Popescu, M. C.; Filip, D.; Vasile, C.; Cruz, C.; Rueff, J. M.; Marcos, M.; Serrano, J. L.; Singurel, G. *J. Phys. Chem. B* **2006**, *110*, 14198–14211.

- (42) Fumino, K.; Wulf, A.; Ludwig, R. *Angew. Chem., Int. Ed.* **2008**, *47*, 3830–3834.
- (43) Kiefer, J.; Fries, J.; Leipertz, A. *Appl. Spectrosc.* **2007**, *61*, 1306–1311.
- (44) Köddermann, T.; Wertz, C.; Heintz, A.; Ludwig, R. *Angew. Chem., Int. Ed.* **2006**, *45*, 3697–3702.